The application of a plant-wide control strategy for an integrated continuous pharmaceutical pilot plant.

Full Paper

The application of an automated control strategy for an integrated continuous pharmaceutical pilot plant

Richard Lakerveld, Brahim Benyahia, Patrick Louis Heider, Haitao Zhang, Aaron Wolfe, Chris Testa, Sean Ogden, Devin R. Hersey, Salvatore Mascia, James Evans, Richard Dean Braatz, and Paul Inigo Barton

Just Accepted

The application of an automated control strategy for

an integrated continuous pharmaceutical pilot plant

Richard Lakerveld,[*,†] *Brahim Benyahia,*[‡] *Patrick L. Heider, Haitao Zhang, Aaron Wolfe, Chris*

Testa, Sean Ogden, Devin R. Hersey, Salvatore Mascia, James M.B. Evans, Richard D. Braatz,

and Paul I. Barton

Department of Chemical Engineering, Massachusetts Institute of Technology, Cambridge,

Massachusetts, USA

ABSTRACT

Continuous manufacturing offers potential opportunities for the improved manufacturing of

pharmaceutical products. A key challenge is the development of an appropriate control strategy.

The experimental application of an automated control strategy is presented for an end-to-end

continuous pharmaceutical pilot plant. The process starts from an advanced intermediate

compound and finishes with the tablet formation steps. The focus of the experimental results is

on the design and performance of the control loops needed to produce a slurry of an active

pharmaceutical ingredient and a solvent with specified material properties. The results

demonstrate that automated control can successfully keep critical material attributes close to

desired set points for a sustained period of operation. This work aims to contribute to the

development of future continuous pharmaceutical processes by providing a realistic case study of automated control of an integrated continuous pharmaceutical pilot plant.

INTRODUCTION

The pharmaceutical industry is challenged by the need for more reliable, cost-effective, and sustainable manufacturing processes. Continuous manufacturing has the potential to provide substantial improvements to pharmaceutical manufacturing compared to traditional batch-wise manufacturing.[1] To facilitate such a transition, research efforts are directed towards understanding and exploiting the potential benefits of operating pharmaceutical unit operations in continuous flow mode such as chemical synthesis in flow,[2] crystallization,[3-5] drying,[6] blending,[7] and roller compaction.[8,9] In addition, system-wide benefits may exist by designing recycle systems to improve the overall yield of the process. Furthermore, process control based on real-time understanding of the dynamic development of final product quality can be harnessed, which in principle allows for corrective action to be taken within the process before large quantities of product go off-spec. As a result, continuous manufacturing may for certain applications reduce batch-to-batch variations, rejection of product, ecological footprint, time-to-market due to easier scale-up, and costs. A recent survey revealed a significant interest in continuous manufacturing from pharmaceutical companies.[10] However, in order for the pharmaceutical industry to embrace fully continuous manufacturing, numerous challenges have to be met. One of these challenges is the design of an integrated plant-wide control strategy.

In order to avoid laborious post-batch testing of product quality, pharmaceutical process development typically defines a so-called *design space,* which is the multi-dimensional space of input variables and process parameters for which the final product has been demonstrated to

meet product quality requirements.[11] The control strategy then focuses on monitoring and possibly controlling the critical process parameters (CPPs) within the design space. Although a design space provides flexibility in the sense that changes to the process within the design space can be implemented directly,[12] distinct challenges exist, which include scale-up and the effort needed to identify the complete design space *a priori* without neglecting attractive regions of operation.[13] The challenge of revealing a sufficiently large design space *a priori* is likely to be more profound for continuous manufacturing as essentially a high-dimensional parameter space is created by linking all process units into a single manufacturing system. On the other hand, if the critical material attributes (CMAs) of streams within the process can be measured online, active feedback control can be employed by using the CPPs as manipulated variables in automated control loops. A strategy of actively controlling CMAs is a more intuitive approach, which is expected to facilitate easier scale-up and would shift the focus of pharmaceutical process development from the documentation of a design space towards development of an active control system.[13] However, in order to apply an approach based on active control of the CMAs, the availability of online process analytical technology (PAT) tools is of crucial importance. In addition, suitable pairings of CMAs with CPPs need to be identified to construct automated control loops. From that perspective, the use of process modeling and process systems engineering tools are of interest to, for example, compute sensitivities of CMAs with respect to CPPs, which can provide a basis for development of a plant-wide control strategy.[9,14,15] A key question that remains is how such a control strategy would perform on a pilot-plant scale for an integrated continuous pharmaceutical process starting from an advanced chemical intermediate to a final tablet in a fully continuous fashion for a realistic pharmaceutical product.

The objective of the current work is to investigate the experimental application of an automated control strategy for an integrated continuous pharmaceutical plant. In prior work, we studied a plant-wide dynamic model of a process, which was inspired by an end-to-end continuous pharmaceutical pilot plant.[16] Subsequently, the model was used to synthesize a plant-wide control structure for the modeled process.[15] Finally, key elements of the synthesized control structure have been translated to an integrated end-to-end continuous pharmaceutical pilot plant. In this paper, we present the experimental performance of this control system at the pilot-plant scale. Although key elements of the control structure that resulted from the model-based design studies have been implemented in the pilot plant, the implemented control structure is not identical to the control structure that was obtained from the model-based studies.[15] For example, features such as recycles that were included in the model-based studies were not implemented in the pilot plant, which simplifies the experimental plant-wide control compared to model-based studies. In general, plant-wide control is a well-studied topic in process control. The main contribution of the current work is the experimental application of known design concepts for plant-wide control to an end-to-end continuous pharmaceutical process.

This paper is part of a series that reports our experimental findings concerning the continuous pharmaceutical pilot plant that has been constructed within the Novartis-MIT Center for Continuous Manufacturing at MIT. The pilot plant produces a pharmaceutical product from start (advanced intermediate) to finish (molded tablets in final dosage form) in a continuous fashion. The produced tablets passed several tests of product quality.[17] This paper presents in detail the design and performance of the control system that was used to produce these tablets. The focus of the experimental results is on the performance of the series of control loops that are needed to produce a slurry of an active pharmaceutical ingredient and a solvent with specified material

properties. A detailed discussion about the design of the pilot plant itself and product quality tests is presented elsewhere.[17] Furthermore, detailed discussions about the design and operation of the chemical synthesis including workup steps and of the continuous crystallization of the API are the subjects of separate papers.[18,19] Finally, a short account of our work has been published in conference proceedings.[20] The focus of the current paper is on the interactions between various control loops and the ability of the control system to maintain key intermediate CMAs close to a desired value in the presence of disturbances both on short and long time scales.

APPROACH

Process and experimental description

The continuous pharmaceutical pilot plant produces tablets with a final dosage of aliskiren hemifumarate as active pharmaceutical ingredient (API). The design of the pilot plant is presented in detail elsewhere[17] and summarized in this section for completeness. The key chemical reactions are given in Scheme 1 and a flowsheet of the plant is given in Figure 1. The process starts by contacting **1** with an excess of **2** in a tubular reactor (R1) with a volume of 2.7 L and in the presence of catalyst **3** at elevated temperature to produce the first intermediate **4**. The conversion of the reaction is equilibrium limited.[21] The reagent **2** and catalyst **3** are dissolved in water and unreacted **1** and **4** are dissolved in ethyl acetate in a mixer (M2). The aqueous phase and organic phase are separated by a membrane device (S1).[22] The intermediate compound **4** is crystallized in two sequential mixed suspension mixed product removal (MSMPR) crystallizers (Cr1,Cr2) for which two 15 L glass vessels with overhead stirrer (Heidolph, RZR 2052) are used. Supersaturation is generated by reducing the temperature and by the addition of an anti-solvent (heptane).[5] The crystals are separated from the mother liquor by

an in-house-made continuous filtration stage (W1). The slurry is distributed on a perforated plate by a weir to create a cake with uniform thickness and ethyl acetate is sprayed on top of the slurry to reduce the amount of mother liquor that adheres to the crystal surface. In addition, ethanol is used to remove traces of water from the slurry to prevent accumulation of water downstream. The filter cake is collected from the plate by a scraper and transported via an auger into a 5 L well-mixed glass vessel (D1) with an overhead stirrer (Heidolph, RZR 2052) to which ethyl acetate is added to reduce the concentration of **4**.

A T-mixer is used to contact the slurry with **4** with aqueous hydrochloric acid to synthesize **5**. The reaction is brought to completion in several minutes in a tubular reactor (R2) at room temperature. The acid is neutralized by adding aqueous sodium hydroxide in an in-line static mixer. The organic phase with **5** is, subsequently, separated from the aqueous phase inside a 5 L glass settler (S3) and diluted with ethyl acetate in a T-mixer downstream of the settler. A number of microfiltration membranes (0.45 μm Pellicon XL 50, Millipore) are installed to retain any solid sodium chloride that may have precipitated (S4). The solubility of the API is known to be water sensitive, so adsorption with 3Å molecular sieves packed in two 35 L dehydration columns (S5) is used to remove traces of water prior to crystallization. At the end of the column, a 1 L glass buffer vessel (B1) is used before the mixture with **5** is mixed with fumaric acid in a 2-stage reactive crystallization (Cr3,Cr4) to crystallize **6** (API).[4,19] The crystallizers are 15 L glass MSMPR crystallizers with an overhead stirrer (Heidolph, RZR 2052). The crystals of API are separated from the mother liquor in a similar continuous washing and filtration stage (W2) as used upstream to filter crystals of **4** before being diluted in a 5 L well-mixed buffer tank (D2) with overhead stirrer (Heidolph, RZR 2052). The slurry with API is mixed with a slurry of silicon dioxide to improve flowability of the dried powder before being fed to a two-stage in-

1
2
3
4
5
6
7
8
9
10
11
12
13
14
15
16
17
18
19
20
21
22
23
24
25
26
27
28
29
30
31
32
33
34
35
36
37
38
39
40
41
42
43
44
45
46
47
48
49
50
51
52
53
54
55
56
57
58
59
60

house-made continuous dryer, which consists of a drum dryer (S6) followed by a tubular dryer

with a rotating screw to convey the powder (S7). Finally, the API powder is mixed with 6000

molecular weight polyethylene glycol in an extruder (Leistritz, Nano16) equipped with two

gravimetric feeders (Schenk, Purefeed DP4). The final tablets are shaped by a custom-made

mold (Mold Hotrunner Solutions) installed at the exit of the extruder (E1).

Scheme 1. Main chemical reactions occurring within the pharmaceutical process leading to the

active pharmaceutical ingredient **6** (adapted from Heider et al.[18]). Compound **7** is a key impurity.

Figure 1. Flowsheet and control structure of the studied continuous pharmaceutical pilot plant. P = Pump, M = Mixer, R = Reactor, S = Separator, Cr = Crystallizer, W = Wash and filtration, D = Dilution tank, B = Buffer tank, E = Extruder, TC = Temperature controller, PC = Pressure controller, CC = Concentration controller, RS = Ratio station, LC = Level controller, PT = Pressure transmitter, FT = Flow rate transmitter, CT = Concentration transmitter, EtOAc = ethyl acetate, HEP = Heptane, EtOH = ethanol, FA = fumaric acid, PEG = polyethylene glycol, CMA = Critical material attribute (see Figures 3, 14, and 12), PU = Purge, FP = Final product. Figure

adapted from Mascia et al.[17] Copyright ©2013 WILEY-VCH Verlag GmbH & Co. KGaA, Weinheim. Printed with permission.

Control strategy and equipment

A schematic representation of the control structure that was implemented in the pilot plant is illustrated in Figure 1. Calibrated volumetric pumps were used to measure and manipulate flow rates. A model-based analysis of a system inspired by the pilot plant[15] is the foundation for the design of the control structure. In general, the control structure consists of a stabilizing and an optimizing control layer. The stabilizing control loops are designed first and consist of all level control loops. Subsequently, optimizing control loops are designed that aim to maintain intermediate CMAs close to desired values. The design of the optimizing control layer is challenging due to: (1) a large number of material attributes that can be controlled, (2) various options to install measurement devices, (3) a large number of variables that can potentially be used as manipulated variables in automated control loops and (4) relevant time scales that span several orders of magnitude within the integrated continuous pharmaceutical process. Fortunately, these challenges to design plant-wide control structures are not unique to pharmaceutical processes and have received considerable attention in the literature for several decades.[23] A hierarchical approach was utilized to develop a plant-wide control strategy based on model-based simulations.[15] The hierarchical approach facilitates decision making and naturally disentangles various time scales, which aims to reduce conflicts between short and long-term control objectives. Several key control loops identified by the model-based studies have been translated to the pilot plant. In order to satisfy long-term product and process requirements, the composition of purified slurry with **4** and API (tanks D1 and D2, respectively) and the corresponding flow rates are identified as key intermediate CMAs and key process requirements,

respectively, which aim to ensure the manufacture of a final product with (1) content of impurity **7** below 0.2%, (2) a nominal mass fraction of API of 0.341, (3) solvent content below 5000 ppm and (4) a desired throughput. An overview of the residence times of each unit operation in the plant is given in Table 1. Note that typical residence times for reactors and separators range from several minutes to several hours with a total residence time of approximately 50 hours for the whole process. A sequential procedure was used for startup in which material out of a certain unit operation was sent to waste first until the quality of the material was constant and close to specification such that feeding to the subsequent unit could commence. Such start-up strategy is expected to shorten the time to steady state at the expense of waste generation during startup.

Table 1. Nominal residence times of unit operations (adapted from Mascia et al.[17])

R1	4	h
S1	<5	min
Cr1	5	h
Cr2	5	h
W1	2	min
D1	2	h
R2	7	min
S3	2	h
S5	15	h
Cr3	4	h
Cr4	4	h
W2	2	min
D2	2	h
S6+7	6	h
E1	12	min

The feed flow rate of **1** is set to a fixed value. Variations in feed flow rate are unmeasured disturbances, which have to be compensated for by the sequence of automated level controllers. The temperature of the first reactor (R1) is maintained constant at elevated temperature in a temperature-controlled oven (130 °C). The pressure of the organic and aqueous flow rate out of the membrane contactor are each controlled by a pressure control valve (Proportion-Air QPV/MPV). The flow rate of organic material leaving the phase separator (S1) is measured by an in-line flow meter (Omega FPR1501), which is used in a feedforward control loop to dose the desired amount of anti-solvent to the subsequent continuous crystallizers. The crystallizers are equipped with feedback temperature control (Thermo Scientific NESLAB RTE Series Refrigerated Bath and Lauda, Proline RP 845 respectively, equipped with a thermocouple and an external Pt-100 resistance thermometer, respectively) and feedback level control (calibrated Omega LVCN414 level sensor). The temperature feedback controllers that use a refrigerated bath are operated locally (actuator not shown in Figure 1). The level controllers aim to maintain stable operation and to minimize variations in flow rate propagating downstream. Therefore, the level controllers of the crystallizers are not tightly controlling the level. Furthermore, the level controllers use proportional control only since a steady-state offset can be tolerated. The tuning of the controller gain provides a maximum outlet pump flow rate when the level in the crystallizer reaches an upper limit, which aims to achieve both stable operation and sufficient flow filtering to reduce variations in flow rate.[24]

The impurities that are propagated to buffer tank D1 have a long-term impact on the overall performance of the process. When the crystals are sufficiently pure, the flow rate of ethyl acetate used for washing (P9) could in principle be used as an actuator in an automated control loop to maintain the level of impurities at a desired set point by removing mother liquor adhering to the

crystalline surface. However, no suitable in-line PAT tool to measure small quantities of key impurities could be identified after an extensive search for our case. Therefore, the flow rate of ethyl acetate was set at a high value to satisfy the required levels of impurities even in the presence of significant disturbances, at the expense of increased solvent usage and reduced yield. Both the outlet flow rate of tank D1 and the concentration of **4** in tank D1 are key intermediate CMAs that have a significant impact on long-term performance of the process. The outlet flow rate of tank D1 is connected to a calibrated level sensor (Omega LVCN414) within a feedback level control loop providing long-term stability and a desired residence time for buffering. Sharp changes in flow rate exiting tank D1 would translate into a strongly varying residence time of the subsequent reaction, which would pose the risk of excessive production of one of the main impurities, eventually causing the final product to go off-spec. Tank D1 acts as a buffer vessel to provide back mixing such that short-term high concentrations of undesired compounds do not propagate. To control the concentration of **4** in the slurry, an on-line density transmitter (Anton Paar DPRn 417) is used to manipulate a solvent flow rate (P11) via feedback control (CC1).

The flow rate of aqueous hydrochloric acid (P13) is ratio controlled with the outlet flow rate of the buffer tank D1 (RS2). Note that the upstream density measurement could be used to adjust the set point of RS2 in case tighter control is required. A feedback control loop (CC2) with an in-line pH probe (Hamilton Polilyte Plus electrode with Omega DP24-PH panel meter) is used to maintain the pH close to a desired set point by using the flow rate of aqueous sodium hydroxide as manipulated variable. A float-type calibrated level sensor (Omega LVR51) is used to measure the position of the liquid-liquid interface in the subsequent settler with an additional calibrated level sensor (Omega LVCN414) mounted in the top of the vessel to measure the total level of the

vessel. Each level sensor is connected to a pump within a level control loop to maintain the holdup of both phases each close to a desired set point.

The concentration of **5** at the inlet of the adsorption column is a local CMA that influences the operation of the crystallization steps downstream. The concentration of **5** in the mixture has to be reduced, which is accomplished by a feedforward flow-rate controller (RS3) to dilute the mixture containing **5** in a fixed ratio using a solvent flow rate (P17) as manipulated variable. Furthermore, an additional outer feedback control loop (CC3) with an in-line ultraviolet (UV) sensor (HR2000+, Ocean Optics) is used in a cascade configuration to adjust the ratio of the flow rates delivered by pumps P16 and P17, which drives the system close to a desired concentration. The dehydration column (S5) contains a conservative amount of molecular sieves, which aims to reject any short-term and long-term disturbances in water content at the inlet of the column by design. The molecular sieves closest to the exit of the column did not saturate during the run, which could be verified via the color of the molecular sieves. The buffer tank at the outlet of the dehydration column is equipped with loosely tuned feedback level control (LC6). The dosage of fumaric acid to synthesize **6** (API) in the subsequent reactive crystallization step (Cr3) is a local CMA related to obtaining the desired product identity and a sufficient yield as the solubility of the API is known to be sensitive to the molar ratio of **5** to fumaric acid in the crystallizers. Therefore, feedforward control (RS4) has been implemented to adjust dosage for disturbances in flow rate and concentration of **5** via an in-line UV sensor (HR2000+, Ocean Optics). The flow rate out of buffer tank B1 is used to set the flow rate of fumaric acid according to a ratio that is optimal for crystallization. The concentration measurement is used to determine the value of this optimal ratio of flow rates.[19] The remaining control loops used for operation of the API crystallizers, combined washing and filtration stage (W12), and buffer tank (D2) are identical to

the crystallizers, washing and filtration device, and buffer tank used for separation of **4** upstream (Cr1, Cr2, W1, D1, respectively).

A flow of a slurry with silicon dioxide (P26) is ratio controlled (RS5) with the outlet flow rate of tank D2 (P25). The first dryer (S6) uses two convection-heated drums for temperature control. The second dryer (S7) uses temperature feedback control with an electrical heating element as actuator (TC6). Furthermore, a number of control valves are installed at the inlet and outlet of the tubular dryer (S7), which open and close in an automated sequence to create an airlock. The screws of the tubular dryer operate at a fixed frequency. The system of automatically operated control valves and feedback temperature controllers allow for continuous uptake of API slurry at the inlet of the dryer and continuous delivery of dried powder at the outlet of the dryer with minimal disturbances to the desired temperatures and pressure for drying. A vacuum conveyor delivers API powder to a gravimetric feeder. The dried powder of API is mixed with polyethylene glycol with two gravimetric feeders, which are operated at a constant feed flow rate. Manual adjustments can be made to regulate the throughput. The mixture of API and excipients are fed into an extruder operated at high temperature to produce a melt of the final dosage. The extruder is equipped with a number of automated temperature controllers to maintain constant temperature in a number of zones.

The nominal set points and tuning parameters of the feedback control loops are given in Table 2 and the nominal set points for the ratio control loops are given in Table 3. All control loops are implemented in a single process control system (Siemens SIMATIC PCS7) equipped with data archiving with the exception of the control loops around the gravimetric feeders and extruder, which are implemented locally.

Table 2. Nominal values for set points and proportional-integral (P(I)) tuning parameters of feedback control loops. The tuning parameters of concentration control loop CC4 were changed during operation according to the given time intervals.

Controller	Set point value	unit	Gain value	unit	Integral time value	unit	comments
LC1	1.05×10^{-2}	m^3	8.3×10^{-4}	s^{-1}	-	-	
LC2	1.15×10^{-2}	m^3	8.3×10^{-4}	s^{-1}	-	-	
LC3	3.00×10^{-3}	m^3	1.7×10^{-3}	s^{-1}	-	-	
LC4	1.20×10^{-3}	m^3	1.7×10^{-2}	s^{-1}	-	-	
LC5	2.65×10^{-3}	m^3	1.7×10^{-3}	s^{-1}	-	-	
LC6	4.00×10^{-4}	m^3	3.3×10^{-3}	s^{-1}	-	-	
LC7	8.00×10^{-3}	m^3	8.3×10^{-4}	s^{-1}	-	-	
LC8	8.00×10^{-3}	m^3	8.3×10^{-4}	s^{-1}	-	-	
LC9	2.50×10^{-3}	m^3	8.3×10^{-4}	s^{-1}	-	-	
CC1	2.62×10^{1}	wt% **4**	2.5×10^{-5}	$m^3 s^{-1}$	-	-	
CC2	1.20×10^{1}	-	7.5×10^{-9}	$m^3 s^{-1}$	50	s	pH
CC3	7.00×10^{0}	wt% **5**	5.1×10^{1}	-	60	s	ratio of RS3
CC4	8.00×10^{0}	wt% **6**	1.7×10^{-4}	$m^3 s^{-1}$	-	-	$t < 147.5$ h
	1.10×10^{1}	wt% **6**	1.7×10^{-4}	$m^3 s^{-1}$	-	-	$147.5 h < t < 169$ h
	1.30×10^{1}	wt% **6**	1.7×10^{-4}	$m^3 s^{-1}$	-	-	$t > 169$ h

Table 3. Nominal set points for ratio control loops

RS1:	FT1/P6	= 1.89
RS2:	P12/P13	= 1.75
RS3:	P17/P16	set by CC3
RS4:	$F_{mol,FA}/F_{mol,\mathbf{5}}$	= 0.5
RS5:	P25/P26	=10.0

RESULTS AND DISCUSSION

This section gives illustrative examples of the performance of the control strategy for the continuous pharmaceutical pilot plant. The integrated pilot plant was run several times. The data presented in this section correspond to a single run of approximately 250 h of sustained operation including start-up and shut-down with a nominal throughput of 41 g h^{-1} of API unless noted otherwise. Results from both long- and short-term performance are presented. Short-term results cover typically a couple of hours, whereas long-term results cover at least a number of days. The experimental run produced data with a typical archiving frequency of 10 sec for each sensor and actuator. To accommodate such a large set of data, characteristic examples are presented by selecting time intervals during the run in which significant disturbances were acting on the system to demonstrate the performance of the critical control loops under challenging conditions. Furthermore, the presented data has been filtered, with details as indicated in the caption of the figures, to reveal only the trends on the process time scales. In general, fluctuations on shorter time scales are also present, for example, due to measurement noise, short-term disturbances, or manual interventions.

The design of an appropriate manufacturing process and control strategy are key parts of a Quality-by-Design approach to pharmaceutical product and process development.[11,12] Both

automated control loops and design decisions that are implemented to maintain CMAs of the process within specification are discussed. First, several examples are given of the impact of disturbances on a number of automated control loops that have a certain hierarchy in priority. Second, the importance of buffering as a design strategy for robust manufacturing is illustrated. Third, an example is given on how the combination of feedback and feedforward control in a cascade configuration can maintain a key intermediate CMA close to a desired value.

Mitigating the effect of disturbances on key intermediate CMAs

To illustrate the interaction between stabilizing and optimizing control loops with different priorities, the performance of several automated control loops in the first part of the plant, which includes the crystallizers Cr1, Cr2, and buffer tank D1, will be discussed in this section. A selection of the control objectives within this part of the plant can be stated in descending order of priority as follows:

1. guarantee long-term stability,

2. maintain the concentration of **1** in buffer tank D1 below a maximum value,

3. maintain the concentration of **4** in buffer tank D1 at a specific value,

4. minimize the variation in outlet flow rate of tank D1,

5. maintain the levels in the crystallizers Cr1 and Cr2 at a desired value,

6. maintain the level in buffer tank D1 at a desired value.

The automated control loops that are implemented to meet these control objectives consists of level control loops LC1, LC2, and LC3, and concentration control loop CC1. First consider the long-term performance of the control loops. The level control loops are part of the stabilizing control layer, which maintain sufficient holdup in each well-mixed vessel over a prolonged

period of time despite a number of significant disturbances during the run as illustrated in Figure 2. The observed variations in level seen in Figure 2 are typically caused by plugging of the tubing around the crystallizers, which has to be resolved manually. In general, plugging of lines and process equipment is an important practical risk for continuous pharmaceutical manufacturing for which early warning systems are important (e.g., via in-line pressure measurements). The concentration and flow rate of the stream leaving buffer tank D1 (P12) are identified from prior model-based studies as key intermediate CMAs that have a long-term impact on the performance of the plant.[15] The concentration of **4** in buffer tank D1 is kept close to a set point by an automated feedback control loop (CC1) for a prolonged period of time as illustrated in Figure 3. The controller has a large gain, which is reflected by a small steady-state offset and a strongly fluctuating flow rate of the solvent feed stream (manipulated variable) as illustrated in Figure 4. This aggressive tuning aims to achieve tight control at the expense of possibly increased wear due to intensive use of the actuator. Furthermore, it can be seen from Figure 4 that towards the end of the run on average less solvent is required to maintain the concentration of **4** close to the set point, which indicates slowly changing performance of upstream units. Possible causes for this observed change in performance could, for example, be a variation in the performance of the filter (e.g., partial plugging of the filter plate) or changing properties of the crystal slurry from crystallizer Cr2 (e.g., in shape, size distribution, or solid content). Nevertheless, the concentration of **4** in buffer tank D1 can be well controlled based on the in-line density meter to the end of the experimental run, which is expected to be of crucial importance to maintain the CMAs of the final product within specification.
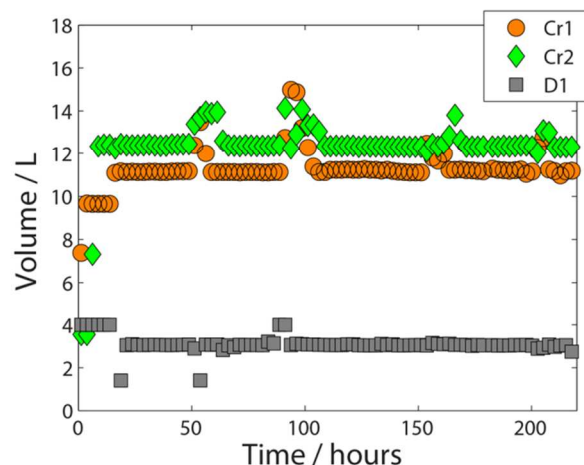
Figure 2. Dynamic development of the measured level in the crystallizers for separation of **4** (Cr1 and Cr2) and the subsequent buffer tank (D1) during 220 h of operation (controlled variables of control loops LC1, LC2, and LC3, respectively). Each point represents the median value of a series of data points collected within 167 min with a sampling frequency of 0.1 Hz.
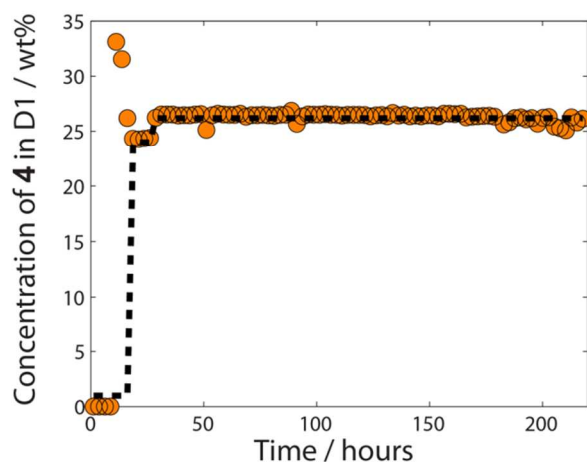

Figure 3. Dynamic development of the concentration of **4** in buffer tank D1 for 220 h of operation (controlled variable of control loop CC1). Each data point represents the median value of a series of data points collected within 150 min with a sampling frequency of 0.1 Hz. The black dashed line represents the set point of the concentration control loop.
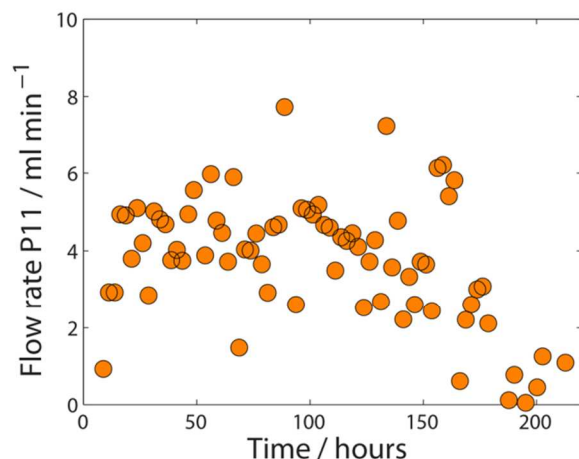
Figure 4. Dynamic development of the flow rate of ethyl acetate fed to buffer tank D1 (P11) for 220 h of operation (manipulated variable of control loop CC1). Each data point represents the median value of a series of data points collected within 150 min with a sampling frequency of 0.1 Hz.

Second, we look at the ability of the automated control loops to mitigate disturbances on a shorter time scale. To that end, a characteristic example of the impact of a significant disturbance that is observed 3 d after startup is presented. The outlet flow rates of crystallizers Cr1 and Cr2 after 72 h of operation are illustrated in Figure 5. Note that these flow rates are manipulated variables in the level control loops around each crystallizer. At the beginning of the time interval, the flow rates are close to steady-state operation. Then the flow from Crystallizer Cr2 to Tank D1 comes to a sudden stop at $t = 72.5$ h due to unintentional plugging of the transfer line between both vessels. Consequently, the level in crystallizer Cr2 quickly rises as illustrated in Figure 6b. Since maintaining the level in Crystallizer Cr2 has low priority, the loose tuning of the feedback level control loop brings the level of the crystallizer back slowly to the set point. Consequently, the effect of the disturbance on the level in buffer tank D1 downstream is limited (Figure 6c). The concentration of **4** in tank D1 drops after the disturbance (Figure 7), which is

mitigated by a quick reduction of the solvent flow rate towards tank D1 (Figure 8). The loose

tuning of the level control loops in the crystallizers and buffer tanks and a more aggressive

tuning of the concentration control loops aim at maintaining the concentration close to a desired

set point while the disturbance in flow rate is diverted towards the level of the crystallizer. In

case sharp changes in the solvent flow rate are not desired from an operational point of view,

integral action could be added to concentration control loop CC1 to reduce the instantaneous and

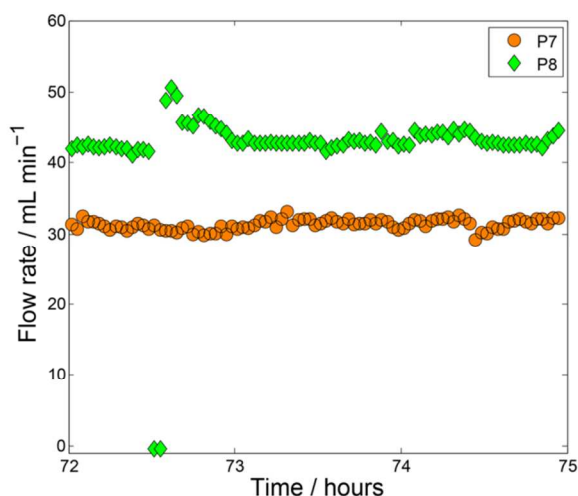step-wise response of a proportional controller.

Figure 5. Dynamic development of the outlet flow rates of crystallizers Cr1 and Cr2 (P7 and P8,

respectively) within a time interval in which a significant disturbance was observed during an

integrated run of an end-to-end continuous pharmaceutical pilot plant (manipulated variables of

control loops LC1 and LC2). Each data point represents the median value of a series of data

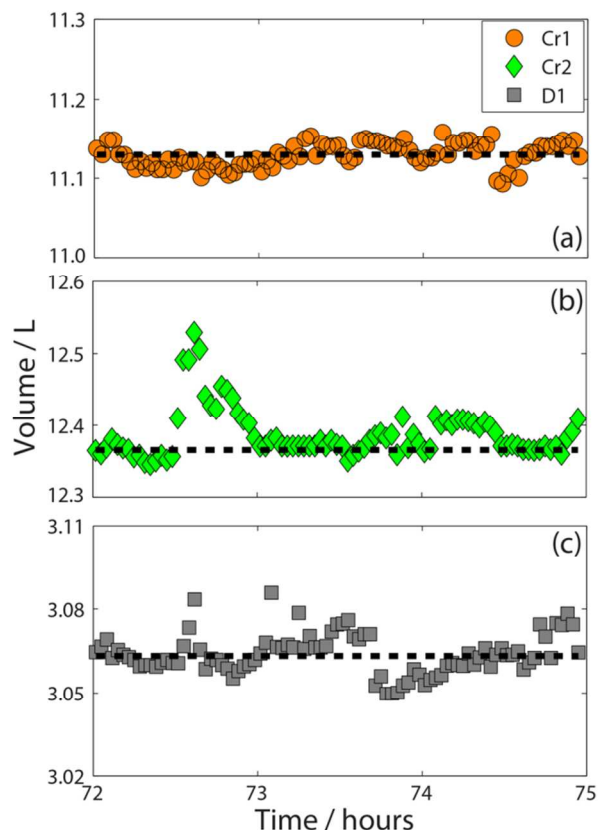points collected within 2 min with a sampling frequency of 0.1 Hz.

Figure 6. Dynamic development of the measured level in the crystallizers for separation of **4** (Cr1 and Cr2) and subsequent buffer tank D1 within a time interval in which a significant disturbance was observed during a run of an end-to-end continuous pharmaceutical pilot plant (controlled variables of control loops LC1, LC2, and LC3, respectively). Each point represents the median value of a series of data points collected within 2 min with a sampling frequency of 0.1 Hz. The black dotted lines represent the set points of the level control loops, which are corrected for a steady-state offset by assuming that the median value of the first 10 data points during the time interval represents the steady-state level in the tanks.
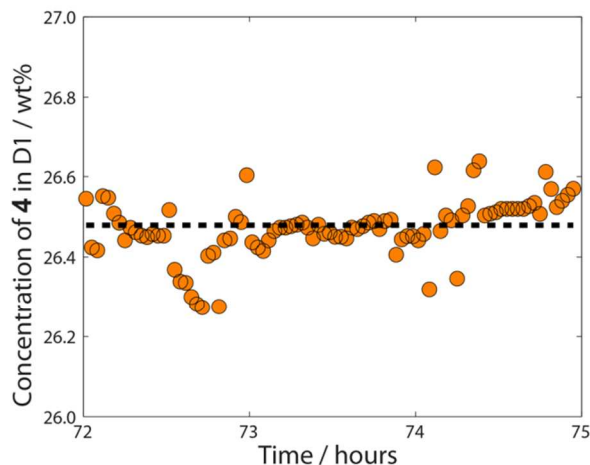
Figure 7. Dynamic development of the concentration of **4** in buffer tank D1 within a time interval in which a significant disturbance was observed during a run of an end-to-end continuous pharmaceutical pilot plant (controlled variable of control loop CC1). Each point represents the median value of a series of data points collected within 2 min with a sampling frequency of 0.1 Hz. The black dotted line represents the set points of the control loop (CC1), which has been corrected for a steady-state offset by assuming that the median value of the first 10 data points during the interval represents the steady-state concentration in the tank.
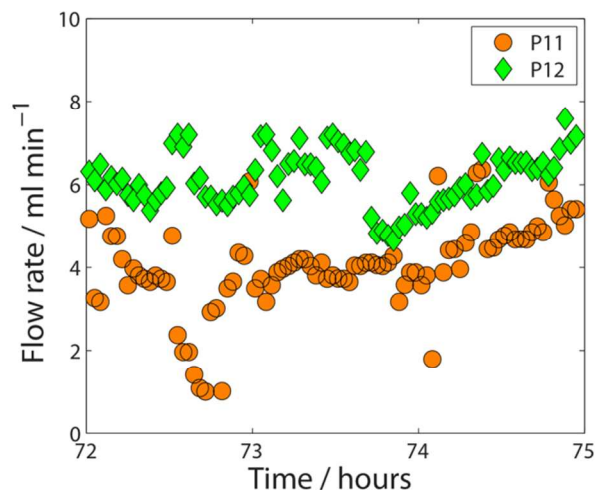
Figure 8. Dynamic development of the flow rate of ethyl acetate fed to buffer tank D1 (P11) and flow rate out of the buffer tank (P12) within a time interval in which a significant disturbance was observed during a run of an end-to-end continuous pharmaceutical pilot plant (manipulated variable of concentration control loop CC1 and manipulated variable of level control loop LC3, respectively). Each point represents the median value of a series of data points collected within 2 min with a sampling frequency of 0.1 Hz.

Figure 9 illustrates a different case, in which a disturbance is observed for several hours that causes the level in crystallizer Cr1 to oscillate (Figure 9a). Such disturbance may be caused by sensor failure or by variations in the flow rates of upstream units. Since the feedback level control loops utilize proportional control only, oscillations in the outlet flow rate of Crystallizer Cr1 are present as well. However, the loose tuning of the level control loop results in relatively small variations in the outlet flow rate of crystallizer Cr1. Consequently, the disturbance and the observed oscillations are strongly reduced in Crystallizer Cr2 (Figure 9b). The dynamic finger print of the disturbance essentially disappears after crystallizer Cr2 (Figure 9c). Instead, a different disturbance can be observed at $t = 132.5$ h in buffer tank D1, which causes the

concentration of **4** in the tank to be higher for several hours (Figure 10). Such sudden increase in

concentration could, for example, be caused by the release of material that accumulated in the

filter device. Since maintaining this concentration has high priority, the flow rate of solvent feed

to tank D1 (the manipulated variable of the automated concentration control loop) increases

sharply (Figure 11) at the expense of an increased volume in buffer tank D1 (Figure 9c) and

outlet flow rate (Figure 11). The present disturbance results in deviations from the set points of

the level and concentration control loops around tank D1 for a longer period of time compared to

the previously discussed disturbance at $t = 72.5$ h (Figures 5 to 8), which indicates a larger

deviation in throughput of compound **4**. Note that the number of reaction equivalents of HCl is

preserved by the automated ratio control loop RS2 (Figure 1). Therefore, the increase in outlet

flow rate of buffer tank D1 will only result in a decrease in residence time of reactor R2. The

number of reaction equivalents of HCl was chosen such that maximum robustness with respect to

changes in throughput was achieved with minimum product degradation.[18] Finally, only

proportional level control was used and it is expected that more advanced control strategies could

further improve the performance of the control loops. For example, model-based studies have

demonstrated for our case that implementation of so-called optimal averaging level control[25] for

buffer tank D1 can reduce significantly variations in outlet flow rate while the performance of

the concentration control loop (CC1) is still satisfactory.[26] Such control strategy aims to

minimize variations in outlet flow rate of a buffer tank while maintaining the level between an

upper and lower boundary instead of at a fixed set point, which for our process would minimize

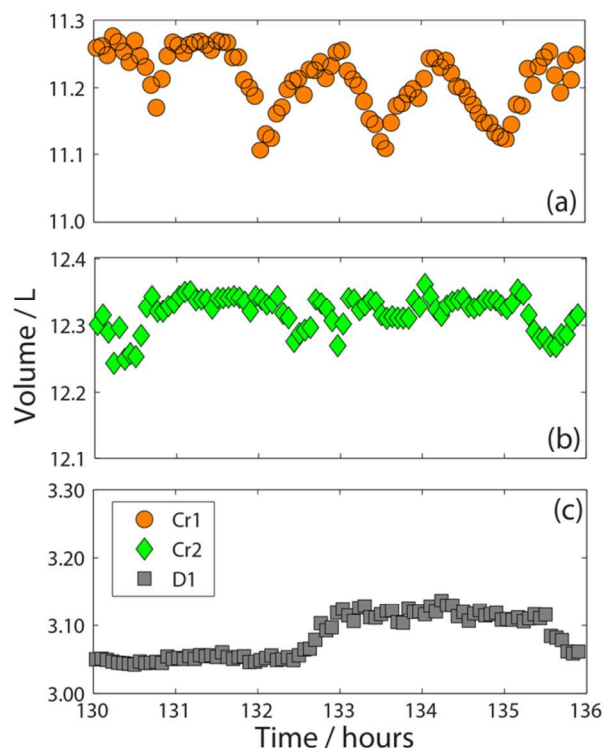variations in the residence time of reactor R2 downstream.

Figure 9. Dynamic development of the measured level in the crystallizers for separation of **4** (Cr1 and Cr2) and subsequent buffer tank D1 within a time interval in which oscillations were observed in the first crystallizer during a run of an end-to-end continuous pharmaceutical pilot plant (controlled variables of control loops LC1, LC2, and LC3, respectively). Each point represents the median value of a series of data points collected within 4 min with a sampling frequency of 0.1 Hz.
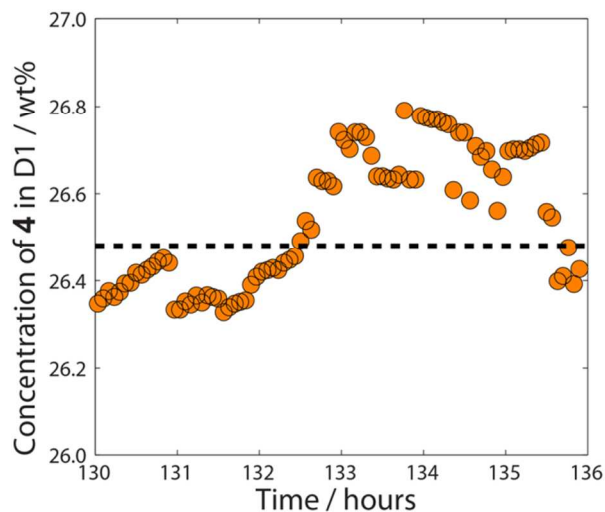
Figure 10. Dynamic development of the concentration of **4** in buffer tank D1 within a time interval in which oscillations were observed in the first crystallizer during a run of an end-to-end continuous pharmaceutical pilot plant (controlled variable of control loop CC1). Each point represents the median value of a series of data points collected within 4 min with a sampling frequency of 0.1 Hz. The black dotted line represents the set points of the control loop (CC1), which has been taken from Figure 7.
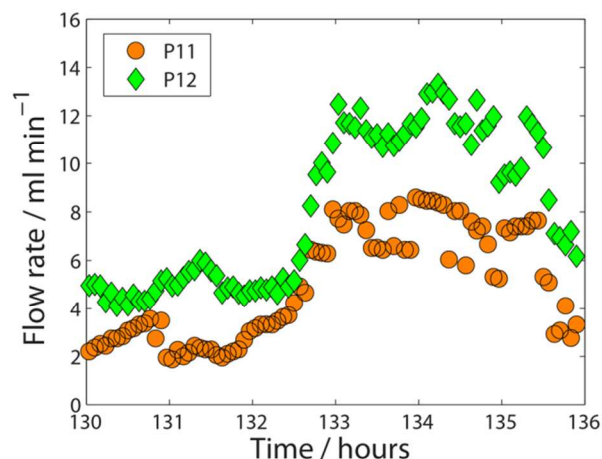
Figure 11. Dynamic development of the flow rate of ethyl acetate fed to buffer tank D1 (P11) and flow rate out of the buffer tank (P12) within a time interval in which a significant disturbance was observed during a run of an end-to-end continuous pharmaceutical pilot plant (manipulated variable of concentration control loop CC1 and manipulated variable of level control loop LC3, respectively). Each point represents the median value of a series of data points collected within 4 min with a sampling frequency of 0.1 Hz.

Further downstream, a similar automated control strategy is used to keep the concentration of **6** (API) in the buffer tank D2 close to a set point. Figure 12 illustrates the concentration of **6** during several days of operation including two changes in the set point of control loop CC4. The figure shows that the control system is well capable to keep the concentration of **6** close to all of the tested set points. Note that there is no active mechanism to increase the concentration in the vessel as the manipulated variable dilutes the slurry. As a result, the system responds slowly when the measured concentration is below the set point and rapidly when the concentration is too high, which can be seen during the set point changes and the disturbance that is shown in the inset of Figure 12. This disturbance was caused by the performance of the filter device upstream, which caused the concentration in the buffer tank D2 to drop over several hours, which

eventually saturated the control loop (i.e., no solvent flow rate into buffer tank D2). The performance of the filter degraded sharply due to a measured loss of vacuum on the permeate side of the filter around $t = 178$ h. The vacuum was restored around $t = 185$ h, which caused the continuous filter device to produce a thicker slurry again. Subsequently, the concentration of **6** increased and solvent was added when the set point was reached, which closed the control loop again and kept the concentration of **6** close to the set point for the remainder of the run.

In summary, the automated control loops in the first part of the pilot plant allowed for production of a slurry with an intermediate compound for a prolonged period of time with CMAs close to desired set points. Close inspection of several observed disturbances during the run demonstrates how disturbances can be diverted from critical to non-critical process parameters (i.e., from flow rate to residence time). A similar control strategy proved to be effective further downstream for the automated control of the concentration of API in the slurry being fed to the continuous drying stage.
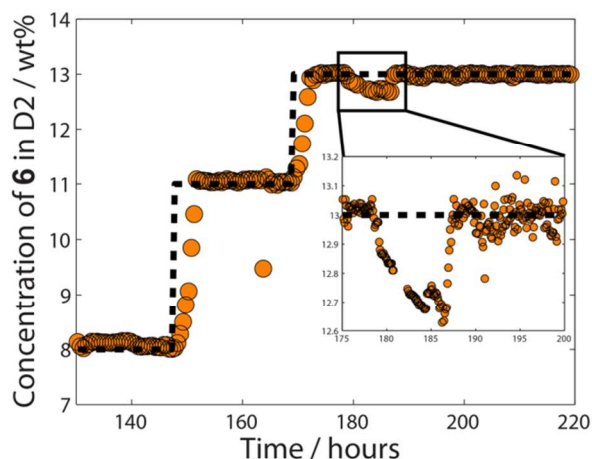

Figure 12. Dynamic development of the concentration of **6** (API) in the buffer tank D2 as obtained from an online density measurement device during several days of operation (controlled variable). The data points represent the median value taken within a measurement period of 30

min with a sampling frequency of 0.1 Hz. The dashed black line represents the set point of the automated concentration control loop (CC4). The inset of the figure illustrates the dynamic development of the concentration during a significant disturbance from upstream in detail (median value taken within 6 min of data collection with a sampling frequency of 0.1 Hz). Note that the control loop is saturated when the measured value of the concentration is below the set point, as there is no active mechanism to increase the concentration.

Mixing to reduce process variability

The concentration of **1** in the slurry leaving buffer tank D1 is an intermediate CMA of the process as the compound is a precursor for the main impurity (**7**) in the final product (Scheme 1).[17] Design strategies can be employed to maintain the concentration at a low value and to prevent strong fluctuations in concentration. First, the solvent flow rate used for washing is set at a high value to meet specifications even in the presence of challenging conditions such as a high slurry load. Second, instead of using a mixing device with a short residence time for dilution, a buffer tank with a residence time of several hours is used, which provides back mixing to dilute material originating from the filter with an overshoot in the concentration of **1**. Throughout most of the run, the fraction of **1** on the filter plate, expressed by HPLC area, shows a similar variation compared to the fraction of **1** within the buffer tank (Figure 13a). Towards the end of the run, the performance of the filter goes down and two events can be detected where temporarily a high fraction of **1** is present on the filter plate. However, the back mixing in the dilution tank prevents propagation of a small quantity of material with high impurity content into units downstream (Figure 13a). Note that the concentration of **1** in the buffer tank steadily goes up towards the end of the run, which is likely caused by propagation of additional mother liquor from the

crystallization steps as the trend coincides with a reduction in solvent addition dictated by concentration control loop CC1 as discussed in the previous section (Figure 4).

The dynamic development of the fraction of the main impurity (**7**) within the slurry on the filter plate W2 and in the dilution tank D2 downstream the process, expressed by HPLC area, is illustrated in Figure 13b. Although less data is available for filter W2 due to the longer time needed to approach steady state for filter W2 compared to filter W1, a similar trend as in Figure 13a can be observed. For most of the measurements, a low fraction of **7** in both the slurry on the filter plate and in the slurry present in dilution tank D2 is measured. However, two events can be noticed when the fraction of impurity within the slurry on the filter plate is significantly higher compared to the slurry in the dilution tank. Such events are unlikely in the dilution tank due to the back mixing, which provides a buffer for propagation of small amounts of material with an excessive high concentration of impurities into the dryer. Note that knowledge on the mixing in all units downstream is required to quantify the acceptable levels of impurity compound **7** at this part of the process. In the period from approximately $t = 135$ h to $t = 152$ h, vacuum was lost at the permeate side of Filter W2 (measured by PT2), which reduced the mother liquor removed and explains the higher fraction of **7** within that period. Once vacuum was restored, filtration performance improved and the impurity level decreased. The fraction of **7** steadily increases towards the end of the run, which may be caused by decreasing performance of the filter or by additional supply of **7** that results from the increasing concentration of **1** in the dilution tank D1 upstream (Figure 13a).
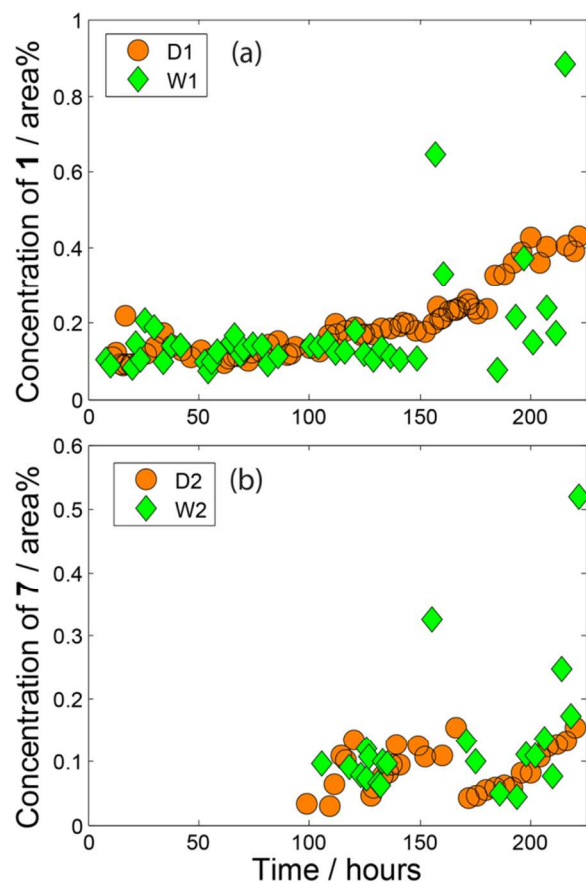
Figure 13. The upper graph, labeled with (a), illustrates the dynamic development of the concentration of **1** in the slurry leaving the filter plate (W1) and in buffer tank D1 during an integrated run of an end-to-end continuous pharmaceutical pilot plant expressed by HPLC area. The bottom graph, labeled with (b), illustrates the dynamic development of the concentration of the main impurity (**7**) in the slurry leaving the filter plate (W2) and in buffer tank D2 downstream. Note that **1** is a precursor for **7** (Scheme 1). Each data point represents, with few exceptions, the average value of two samples. Measurements that could not be reproduced are removed from the data set.

Combined feedforward and feedback in cascade control loops

Feedforward control has the ability to reject disturbances before a controlled variable is affected. One of the most common forms of feedforward control is *ratio control*, which typically involves specifying the flow rate for one stream as a ratio of the measured flow rate of another stream. In contrast, feedback control relies on deviations of a controlled variable from a set point, which has the advantage of keeping the controlled variable close to its desired set point. A configuration that combines ratio control with feedback control is *ratio cascade control*,[27] in which an outer feedback control loop manipulates the ratio in an inner ratio control loop. This section demonstrates the importance of this strategy for the integrated continuous pharmaceutical pilot plant with an example to maintain a CMA of a process stream close to a desired set point in the presence of fast and slow disturbances. The control loops of interest (RS3,CC3) are installed around settler S3 and dehydration column S5 (Figure 1). A liquid with **5** dissolved in an organic phase is separated from an aqueous phase and fed into a dehydration column after dilution. The concentration of **5** has to be maintained close to a desired set point before entering the dehydration column. Typical disturbances that can be expected are variations in the flow rate and concentration of the mixture from the settler. The impact of variations in flow rate on the concentration after dilution can be mitigated by manipulating the flow rate of the solvent feed stream with a ratio control loop (inner feedforward loop). Furthermore, an outer feedback control loop ensures that the concentration after dilution is close to a desired set point by manipulating the set point of the ratio control loop, which mitigates variations in the concentration of the mixture from the settler.

The feedback concentration control loop is complicated by a significant delay time between the mixing point and the UV sensor, because possible salt crystals have to be removed first after

mixing to obtain a signal of sufficient quality from the UV sensor. An appropriate tuning of the control parameters that takes into account this delay time is of crucial importance. Therefore, prior to the run, two process reaction curves[24] were experimentally measured by applying step inputs of the set point of ratio controller RS3 from which the effective delay time, the process time constant, and the steady-state gain were estimated. Subsequently, recommended tuning parameters,[28,29] which are based on the Internal Model Control design method,[30,31] were used to obtain an estimated value for the controller gain and integral time of controller CC3.

To compare the performance of feedforward control alone with the performance of the combined feedforward and feedback control loop, two sets of data from different experimental runs are compared. In both cases, a time interval of 20 consecutive hours was selected in which the main control loops upstream are all closed. Figure 14a illustrates the concentration of **5** before entering the dehydration column when only the feedforward control loop is implemented (i.e., with a fixed set point for the ratio control loop). In contrast, Figure 14b shows the same concentration from the run where both the feedforward and feedback control loops are combined in an automated cascade control loop. The figure shows that, at least for the illustrated time interval, slow variations in concentration are observed when only feedforward control is implemented and a more uniform concentration is achieved when feedforward and feedback control are combined. Note that several outliers can be observed in the measured data, which are likely the result of temporary manual operation to clean the salt filters (S4) upstream of the UV measurement device. In the case of Figure 14a, no set point for the concentration can be set, which complicates the optimization of downstream units and may result in a persistent drift in concentration during a sustained period of operation. In contrast, adding an outer feedback control loop allows for the concentration to be kept close to a set point.
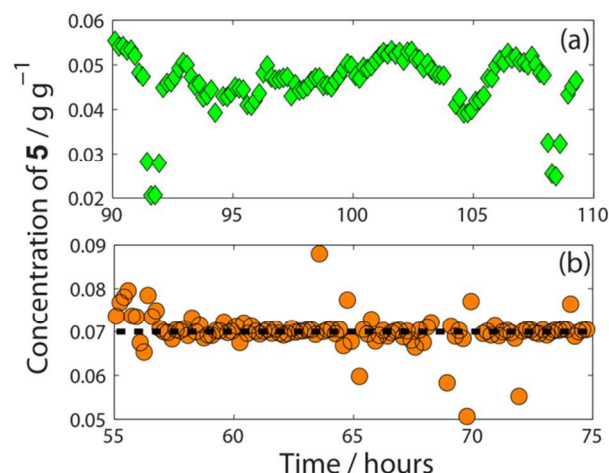
Figure 14. Dynamic development of the concentration of **5** after dilution and before entering the dehydration column (S5) for a representative time interval. The upper graph, labeled with (a), is taken from a different run compared to the bottom graph, labeled with (b), in which a different control strategy was tested. The upper graph is from a run in which the outer concentration feedback control loop (CC3) was not implemented and only a feedforward ratio controller (RS3) was used. The lower graph corresponds to a run in which both the outer concentration feedback control loop (CC3) and inner ratio control loop (RS3) were implemented in a cascade configuration. The black dashed line represents the set point of the outer loop. The data points in both (a) and (b) represent the median value taken within 10 min of data collection with a sampling frequency of 0.1 Hz.

CONCLUSIONS

The experimental application of an automated control strategy is presented for an end-to-end continuous pharmaceutical pilot plant. The results demonstrate the ability to control critical material attributes (CMAs) related to the properties of slurries with an intermediate compound or the active pharmaceutical ingredient for a sustained period of operation at least for the tested

conditions, which included set point changes. Detailed inspection of the performance of several control loops within shorter time intervals reveal insights about the interaction between automated control loops, the importance of buffering, and the performance of a combined feedforward and feedback cascade control. In particular, the interaction of several automated level control loops and a concentration control loop around two continuous crystallization units, filter, and buffer tank shows the diversion of key disturbances to non-critical process parameters. The filtered slurry can contain relatively small amounts of material with a high impurity content, which can be mitigated via back mixing in a buffer tank. In general, back mixing has an impact on the dynamics of product quality and, for example, poses challenging questions for a sampling strategy. Therefore, there is an increased need to understand the impact of residence time distribution for continuous pharmaceutical manufacturing.[32] Finally, comparison of the performance of a concentration control loop with only feedforward control and the same concentration control loop with combined feedforward and feedback control clearly demonstrates the effectiveness of the latter strategy for tight control of an intermediate CMA within the process.

The experimentally tested control strategy consisted only of conventional feedback and feedforward automated control loops. However, it is expected that advanced control strategies such as model-predictive control (MPC) would offer significantly improved control performance as was recently demonstrated for our application via model-based studies.[33] In addition, the benefits of MPC have been demonstrated clearly for other configurations of continuous pharmaceutical processes via model-based studies such as a continuous pharmaceutical tablet manufacturing process via direct compaction.[34] A key advantage of MPC is that process constraints can be taken into account explicitly. Experimental implementation of MPC requires a

validated process model, which could also be used to investigate the allowable variation in controlled variables in a quantitative way. In addition, process models can be used to investigate the impact of residence time distribution of a train of unit operations on the final product quality. Advanced control strategies and dynamic process models for continuous pharmaceutical manufacturing provide in general interesting directions for future research.

AUTHOR INFORMATION

Corresponding Author

* E-mail: r.lakerveld@tudelft.nl, Tel:+31152783852.

Present Addresses

† Department of Process & Energy, Delft University of Technology, Delft, The Netherlands.

‡ Department of Chemical Engineering, Loughborough University, Loughborough, UK

Author Contributions

The manuscript was written through contributions of all authors. All authors have given approval to the final version of the manuscript.

REFERENCES

(1)　a) Schaber, S.D.; Gerogiorgis, D.I.; Ramachandran, R.; Evans, J.M.B.; Barton, P.I.; Trout, B.L. *Ind. Eng. Chem. Res.* **2011**, *50*, 10083-10092. b) Plumb, K. *Chem. Eng. Res. Des.* **2005**, *83*, 730-738. c) Roberge, D.M.; Ducry, L.; Bieler, N.; Cretton, P.; Zimmermann, B. *Chem. Eng. Technol.* **2005**, *28*, 318-323. d) Roberge, D.M.; Zimmermann, B.; Rainone, F.; Gottsponer, M.; Eyholzer, M.; Kockmann, N. *Org. Process Res. Dev.* **2008**, *12*, 905-910. e) Jimenez-Gonzalez, C.; Poechlauer, P.; Broxterman, Q.B.; Yang, B.S.; Am Ende, D.; Baird, J.; Bertsch, C.; Hannah, R.E.; Dell'Orco, P.; Noorrnan, H.; Yee, S.; Reintjens, R.; Wells, A.; Massonneau, V.; Manley, J. *Org. Process. Res. Dev.* **2011**, *15*, 900-911. f) LaPorte, T.L.; Wang, C. *Curr. Opin. Drug Discovery Dev.* **2007**, *10*, 738-745.

(2)　a) Kockmann, N.; Gottsponer, M.; Zimmermann, B.; Roberge, D.M. *Chem. Eur. J.* **2008**, *14*, 7470-7477. b) Hartman, R.L.; McMullen, J.P.; Jensen, K.F. *Angew. Chem. Int. Ed.* **2011**, *50*, 7502-7519. c) Wegner, J.; Ceylan, S.; Kirschning, A. *Chem. Commun.* **2011**, *47*, 4583-4592. d) Wegner, J.; Ceylan, S.; Kirschning, A. *Adv. Synth. Catal.* **2012**, *354*, 17-57. e) Wiles, C.; Watts, P. *Green Chem.* **2012**, *14*, 38-54. f) Pollet, P.; Cope, E.D.;

Kassner, M.K.; Charney, R.; Terett, S.H.; Richman, K.W.; Dubay, W.; Stringer, J.; Eckertt, C.A.; Liotta, C.L. *Ind. Eng. Chem. Res.* **2009**, *48*, 7032-7036. g) Christensen, K.M.; Pedersen, M.J.; Dam-Johansen, K.; Holm, T.L.; Skovby, T.; Kiil, S. *Chem. Eng. Sci.* **2012**, *26*, 111-117.

(3) a) Chen, J.; Sarma, B.; Evans, J.M.B.; Myerson, A.S. *Cryst. Growth Des.* **2011**, *11*, 887-895. b) Griffin, D.W.; Mellichamp, D.A.; Doherty, M.F. *Chem. Eng. Sci.* **2010**, *65*, 5770-5780. c) Wong, S.Y.; Tatusko, A.P.; Trout, B.L.; Myerson, A.S. *Cryst. Growth Des.* **2012**, *12*, 5701-5707. d) Alvarez, A.J.; Myerson, A.S. *Cryst. Growth Des.* **2010**, *10*, 2219-2228. e) Alvarez, A.J.; Singh, A.; Myerson, A.S. *Cryst. Growth Des.* **2011**, *11*, 4392-4400. f) Lawton, S.; Steele, G.; Shering, P.; Zhao, L.H.; Laird, I.; Ni, X.W. *Org. Process Res. Dev.* **2009**, *13*, 1357-1363. g) Eder, R.J.P.; Schmitt, E.K.; Grill, J.; Radl, S.; Gruber-Woelfler, H.; Khinast, J.G. *Cryst. Res. Technol.* **2011**, *46*, 227-237. h) Eder, R.J.P.; Schrank, S.; Besenhard, M.O.; Roblegg, E.; Gruber-Woelfler, H.; Khinast, J.G. *Cryst. Growth Des.* **2012**, *12*, 4733-4738. i) Ferguson, S.; Morris, G.; Hao, H.; Barrett, M.; Glennon, B. *Chem. Eng. Sci.* **2013**, *104*, 44-54. j) Zhao, L.; Raval, V.; Briggs, N.; Bhardwaj, R.M.; McGlone, T.; Oswald, I.D.H.; Florence, A.J. *Crystengcomm* **2014**, *16*, 5769-5780.

(4) Quon, J.; Zhang, H.; Alvarez, A.J.; Evans, J.M.B.; Myerson, A.S.; Trout, B.L. *Org. Process Res. Dev.* **2012**, *12*, 3036-3044.

(5) Zhang, H,; Quon, J.; Alvarez, A.J.; Evans, J.M.B.; Myerson, A.S.; Trout, B.L. *Org. Process Res. Dev.* **2012**, *16*, 915-924.
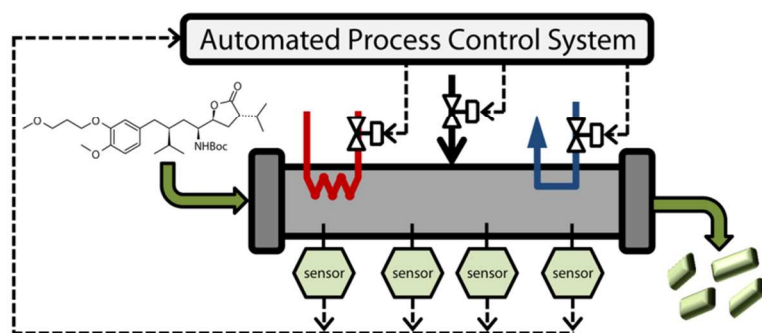
(6)   a) Mortier, S.T.F.C.; De Beer, T.; Gernaey, K.V.; Vercruysse, J.; Fonteyne, M.; Remon, J.P.; Vervaet, C.; Nopens, I. *Eur. J. Pharm. Biopharm.* **2012**, *80*, 682-689. b) Gonnissen, Y.; Remon, J.P.; Vervaet, C. *Eur. J. Pharm. Biopharm.* **2007**, *67*, 220-226. c) Gonnissen, Y.; Goncalves, S.I.V.; De Geest, B.G.; Remon, J.P.; Vervaet, C. *Eur. J. Pharm. Biopharm.* **2008**, *68*, 760-770. d) Wang, M.; Rutledge, G.C.; Myerson, A.S.; Trout, B.L. *J. Pharm. Sci.* **2012**, *101*, 1178-1188. e) Brettmann, B.; Bell, E.; Myerson, A.S.; Trout, B.L. *J. Pharm. Sci.* **2012**, *101*, 1538-1545. f) Brettmann, B.K.; Cheng, K.; Myerson, A.S.; Trout, B.L. *Pharm. Res.* **2013**, *30*, 238-246.

(7)   a) Dubey, A.; Vanarase, A.U.; Muzzio, F.J. *AIChE J.* **2012**, *58*, 3676-3684. b) Dubey, A.; Sarkar, A.; Ierapetritou, M.; Wassgren, C.R.; Muzzio, F.J. *Macromol. Mater. Eng.* **2011**, *296*, 290-307. c) Portillo, P.M.; Ierapetritou, M.; Muzzio, F.J. *Powder Technol.* **2009**, *194*, 217-227.

(8)   Hamdan, I.M.; Reklaitis, G.V.; Venkatasubramanian, V. *J. Pharm. Innov.* **2010**, *5*, 147-160.

(9)   Singh, R.; Ierapetritou, M.; Ramachandran, R. *Int. J. Pharm.* **2012**, *438*, 307-326.

(10)   Poechlauer, P.; Manley, J.; Broxterman, R.; Gregertsen, B.; Ridemark, M. *Org. Process Res. Dev.* **2012**, *16*, 1586-1590.

(11)   ICH. Guidance for Industry Q8(R2) Pharmaceutical Development. U.S. Food and Drug Administration, Silver Spring, Maryland, November 2009.

(12)   Yu, L.X. *Pharm. Res.* **2008**, *25*, 781-791.

(13) Lionberger, R.A.; Lee, S.L.; Lee, L.; Raw, A.; Yu, L.X. *The AAPS Journal* **2008**, *10*, 268-276.

(14) a) Singh, R.; Gernaey, K.V.; Gani, R. *Comput. Chem. Eng.* **2009**, *33*, 22-42. b) Gernaey, K.V.; Cervera-Padrell, A.E.; Woodley, J.M. *Comput. Chem. Eng.* **2012**, *42*, 15-29. c) Cervera-Padrell, A.E.; Skovby, T.; Kiil, S.; Gani, R.; Gernaey, K.V. *Eur. J. Pharm. Biopharm.* **2012**, *82*, 437-456. d) Gernaey, K.V.; Gani, R. *Chem. Eng. Sci.* **2010**, *65*, 5757-5769. e) Gernaey, K.V.; Cervera-Padrell, A.E.;Woodley, J.M. *Future Med. Chem.* **2012**, *4*, 1371-1374. f) Boukouvala, F.; Niotis, V.; Ramachandran, R.; Muzzio, F.J.; Ierapetritou, M.G. *Comput. Chem. Eng.* **2012**, *42*, 30-47. g) Sen, M.; Rogers, A.; Singh, R.; Chaudhury, A.; John, J.; Ierapetritou, M.G.; Ramachandran, R. *Chem. Eng. Sci.* **2013**, *102*, 56-66.

(15) Lakerveld, R.; Benyahia, B.; Braatz, R.D.; Barton, P.I. *AIChE J.* **2013**, *59*, 3671-3685.

(16) Benyahia, B.; Lakerveld, R.; Barton, P.I. *Ind. Eng. Chem. Res.* **2012**, *51*, 15393-15412.

(17) Mascia, S.; Heider, P.L.; Zhang, H.; Lakerveld, R.; Benyahia, B.; Barton, P.I.; Braatz, R.D., Cooney, C.L.; Evans, J.M.B.; Jamison, T.F.; Jensen, K.F.; Myerson, A.S.; Trout, B.L. *Angew. Chem. Int. Ed.* **2013**, *52*, 12359-12363.

(18) Heider, P.L.; Born, S.C.; Basak, S.; Benyahia, B.; Lakerveld, R.; Zhang, H.; Hogan, R.; Buchbinder, L.; Wolfe, A.; Mascia, S.; Evans, J.M.B.; Jamison, T.F.; Jensen, K.F. *Org. Process Res. Dev.* **2014**, *18*, 402-409.

(19) Zhang, H.; Lakerveld, R.; Heider, P.L.; Tao, M.; Su, M.; Testa, C.J.; D'Antonio, A.N.; Barton, P.I.; Braatz, R.D.; Trout, B.L.; Myerson, A.S.; Jensen, K.F.; Evans, J.M.B. *Cryst. Growth Des.* **2014**, *14*, 2148–2157.

(20) Lakerveld, R.; Benyahia, B.; Heider, P.L.; Zhang, H.; Wolfe, A.; Testa, C.; Ogden, S.; Hersey, D.R.; Mascia, S.; Evans, J.M.B.; Braatz, R.D.; Barton, P.I. *Proceedings of the 2014 American Control Conference* **2014**, Portland, Oregon, USA, 3512-3517.

(21) Foley, M.A.; Jamison, T.F. *Org. Process Res. Dev.* **2010**, *14*, 1177-1181.

(22) Kralj, J.G.; Sahoo, H.R.; Jensen, K.F. *Lab Chip* **2007**, *7*, 256-263.

(23) a) Buckley, P.S. *Techniques of Process Control*; John Wiley & Sons:New York, 1964. b) Morari, M.; Arkun, Y.; Stephanopoulos, G. *AIChE J.* **1980**, *26*, 220-232. c) Morari, M.; Stephanopoulos, G. *AIChE J.* **1980**, *26*, 232-246. d) Larsson, T.; Skogestad, S. *Int. J. Model. Ident. Control* **2000**, *21*, 209-240. e) Stephanopoulos, G.; Ng, C. *J. Process Control* **2000**, *10*, 97-111.

(24) Seborg, D.E.; Edgar, T.F.; Mellichamp, D.A.; Doyle III, F.J. *Process Dynamics and Control (3rd edition)*; John Wiley & Sons:Hoboken, New Jersey, 2011, 107-108.

(25) McDonald, K.A.; McAvoy, T.J.; Tits, A. *AIChE J.* **1986**, 32, 75-86.

(26) Lakerveld, R.; Benyahia, B.; Heider, P.L.; Zhang, H.; Braatz, R.D.; Barton, P.I. *Processes* **2013**, *1*, 330-348.

(27) Smith, C. *Practical Process Control: Tuning and Troubleshooting*; John Wiley & Sons:Hoboken, New Jersey, 2009, 365-368.

(28) Lin, M.G.; Lakshminarayanan, S.; Rangaiah, G.P. *Ind. Eng. Chem. Res.* **2008**, *47*, 344-368.

(29) Skogestad, S. *J. Process Contr.* **2003**, *13*, 291-309.

(30) Garcia, C.E.; Morari, M. *Ind. Eng. Chem. Process Des. Dev.* **1982**, *21*, 308.

(31) Rivera, D.E.; Morari, M.; Skogestad, S. *Ind. Eng. Chem. Process Des. Dev.* **1986**, *25*, 252.

(32) Chatterjee, S. *FDA Perspective on Continuous Manufacturing*, presented at the 2012 IFPAC Annual Meeting, Baltimore, MD.

(33) Mesbah, A.; Lakerveld, R.; Braatz, R.D. *Plant-Wide Model Predictive Control of a Continuous Pharmaceutical Manufacturing Process*, presented at the 2013 AIChE Annual Meeting, San Francisco, CA.

(34) Singh, R.; Ierapetritou, M.; Ramachandran, R. *Eur. J. Pharm. Biopharm.* **2013**, *85*, 1164-1182.

SYNOPSIS

For Table of Contents Only